SCIENTIFIC REPORTS

OPEN

Classical and quantum conductivity in β-Ga_2O_3

David C. Look[1,2] & Kevin D. Leedy[2]

Received: 16 August 2018
Accepted: 19 December 2018
Published online: 04 February 2019

The conductivity σ, quantum-based magnetoconductivity $\Delta\sigma = \sigma(B) - \sigma(0)$, and Hall coefficient R_H ($= \mu_H/\sigma$) of degenerate, homoepitaxial, (010) Si-doped β-Ga_2O_3, have been measured over a temperature range T = 9–320 K and magnetic field range B = 0–10 kG. With ten atoms in the unit cell, the normal-mode phonon structure of β-Ga_2O_3 is very complex, with optical-phonon energies ranging from kT_{po} ~ 20–100 meV. For heavily doped samples, the phonon spectrum is further modified by doping disorder. We explore the possibility of developing a single function $T_{po}(T)$ that can be incorporated into both quantum and classical scattering theory such that Δσ vs B, Δσ vs T, and μ_H vs T are all well fitted. Surprisingly, a relatively simple function, $T_{po}(T) = 1.6 \times 10^3\{1 - \exp[-(T+1)/170]\}$ K, works well for β-Ga_2O_3 without any additional fitting parameters. In contrast, Δσ vs T in degenerate ScN, which has only one optical phonon branch, is well fitted with a *constant* $T_{po} = 550$ K. These results indicate that quantum conductivity enables an understanding of classical conductivity in disordered, multi-phonon semiconductors.

The semiconductor Ga_2O_3 has five structural forms, α, β, γ, δ, and ε, the most stable of which is β-Ga_2O_3 (hereafter called βGAO), which crystallizes in the monoclinic form. This material has experienced extensive research activity in the last few years, mainly because of its high band gap, $E_g = 4.6$–4.9 eV, significantly higher than that of most other common wide-band-gap semiconductors, such as GaN, ZnO, and SiC[1,2]. This feature leads to a higher breakdown field[3], important for power electronics, and also less absorption in the UV, useful for applications requiring transparency[2]. Moreover, even with this large band gap, βGAO can be highly doped with shallow donors such as Si and Sn, attaining free-electron concentrations $n \approx 2 \times 10^{20}$ cm^{-3} [4]. Such high concentrations enable transparent electrodes for photovoltaics and flat-panel displays, and regrown ohmic contacts[5]. Finally, homoepitaxial device technology is possible because large βGAO crystals can be grown by several different techniques[2].

With such interesting practical applications on the horizon, it is important to understand the classical electrical properties, in particular, conductivity σ, concentration n, and Hall mobility $\mu_H = \sigma R_H$, where R_H is the Hall coefficient. For binary semiconductors with only two atoms in the unit cell, such as GaN, SiC, ZnO, and ScN, the relevant scattering theory is simplified by the existence of only one branch of optical phonons. Thus, polar-optical-phonon scattering in these materials can be effectively described in terms of only one longitudinal optical phonon, of energy kT_{po}[6], where k is Boltzmann's constant and T_{po} is the polar optical phonon temperature. (For reference, the table on p. 84 of[6] lists T_{po} values for sixteen binary semiconductors.) In contrast, βGAO contains ten atoms in the unit cell and thus nine branches of optical phonons, greatly complicating the analysis. The full spectrum of normal-mode phonons has recently been calculated and discussed in detail[7–10]. However, in this study, we will be concerned with *degenerate* Si-doped βGAO, which has the additional complication of disorder due to the random positions of the Si-dopant atoms[11–13]. Such disorder leads to small, negative contributions to the conductivity via a quantum effect, electron-wave constructive interference. This effect can be reduced by an increase in temperature T or magnetic-field strength B, with the latter leading to a positive magnetoconductivity (MC). We define $\Delta\sigma(B,T) = \sigma(B,T) - \sigma(0,T)$, and will show that a theoretical analysis of Δσ as a function of B and T provides enough detail of the actual phonon spectrum to quantitatively explain μ_H vs T, a completely different experiment. Besides this *positive* contribution to the MC, a much more common, non-quantum, *negative* contribution to the MC can also exist[11–14]; however, it is negligible in our sample due to a high degree of degeneracy.

The film of this study was homoepitaxial, grown by pulsed laser deposition (PLD) at 550 °C on a Fe-doped (010) βGAO substrate. The substrate was semi-insulating and thus electrically isolated from the film. The growth ambient was a 5% O_2/95% Ar gas mixture at 1.33 Pa, and the ablation target was a 99.99% pure sintered Ga_2O_3

[1]Semiconductor Research Center, Wright State University, Dayton, OH, 45435, USA. [2]Air Force Research Laboratory Sensors Directorate, Wright-Patterson AFB, OH, 45433, USA. Correspondence and requests for materials should be addressed to D.C.L. (email: david.look@wright.edu)

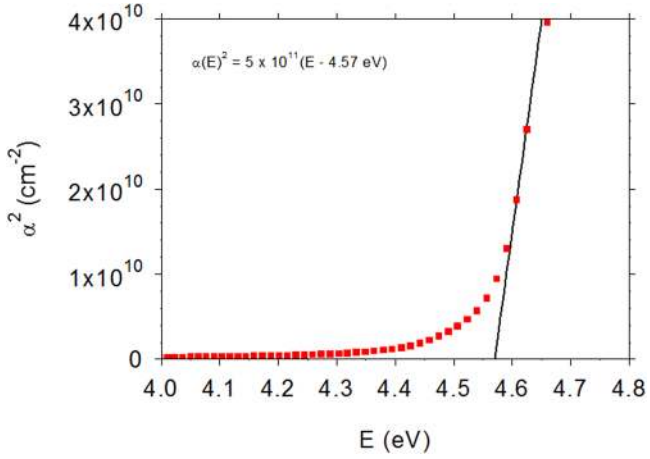

Figure 1. Square of absorption coefficient α vs energy E for βGAO. The intercept of α^2 vs E gives a direct energy gap of 4.57 eV.

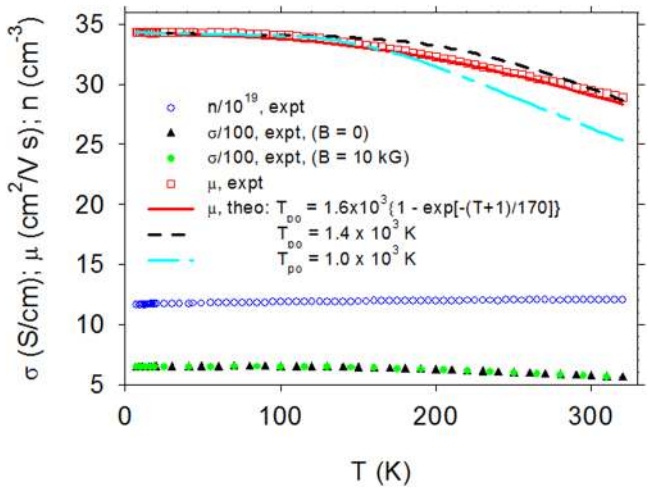

Figure 2. Conductivity σ, Hall-mobilty μ, and free-electron concentration n, vs temperature T in βGAO. The lines are theoretical fits of μ vs T under three possible conditions: (1) $T_{po}(T) = 1.4 \times 10^3$ K; (2) $T_{po}(T) = 1.0 \times 10^3$ K; or (3) $T_{po}(T) = 1.6 \times 10^3\{1 - \exp[-(T+1)/170]\}$ K.

disk with 1 wt. % SiO_2. Nearly identical films have been extensively characterized by X-ray diffraction (XRD), atomic-force microscopy (AFM), and transmission electron microscopy (TEM), as presented in ref.[4]. A film thickness d = 502 nm was measured by contact profilometry. The thickness was also determined from spectral reflectance R_m and transmittance T_m measurements which can be accurately converted to the elements η and κ of the index of refraction (η + iκ) in a homoepitaxial sample[15]. At an energy E = 2 eV, η = 2.02, and Fabry-Perot oscillations (FPO) then yielded d = 508 nm, close to the profilometer value.

Another common use of R_m and T_m measurements is determination of the band gap E_g[15]. The values of η and κ can be directly converted to absorption α and reflection R coefficients, and for crystalline materials with a direct band gap, a plot of α^2 vs energy E will have an intercept E_g at E = 0. As shown in Fig. 1, the result is: $\alpha^2 = 5 \times 10^{11}$ (E − 4.57 eV) cm^{-2}, giving $E_g = 4.57$ eV. In agreement, typical E_g values for βGAO mentioned in the literature are 4.5–4.9 eV[1].

Measurements of sheet carrier concentration n_s, sheet conductance σ_s, and sheet Hall coefficient R_{Hs} were carried out in a LakeShore 7507 Hall-effect system over a temperature range T = 9–320 K and a magnetic-field range, B = 0–10 kG. (All of the numbered equations in this work are in MKS units. However, in the text we will report B in "kG" rather than in the MKS unit "T" because "T" is already used for temperature. Note that 10 kG = 1 T.) For comparison with theory, σ_s was converted to conductivity $\sigma = \sigma_s/d$, R_{Hs} to volume electron concentration $n = (edR_{Hs})^{-1}$, and Hall mobility to $\mu_H = \sigma_s R_{Hs}$[14]. Plots of n, μ_H, and σ vs T are shown in Fig. 2. (Note that because n is nearly constant at 1.2×10^{20} cm^{-3}, the layer is degenerate, and the so-called "Hall factor" is thus close to unity; in such a case, n is the true carrier concentration[14]) In Fig. 2, we have plotted σ at both B = 0 and B = 10 kG. Although the curves appear to be nearly identical on the scale of this plot, their small difference Δσ is important and is expanded and plotted vs temperature in Fig. 3.

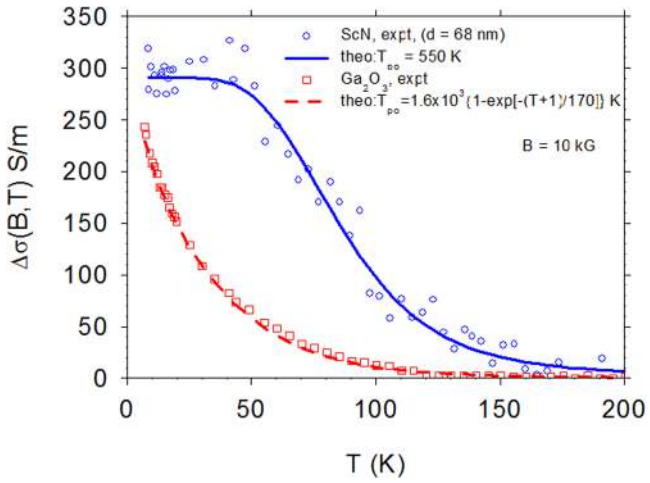

Figure 3. Magnetoconductivity $\Delta\sigma$ vs T, B = 10 kG, for βGAO and thin-film ScN. The ScN is well fitted with a constant $T_{po} = 550$ K, but the βGAO requires a function $T_{po}(T) = 1.6 \times 10^3\{1 - \exp[-(T+1)/170]\}$ K.

As mentioned earlier, the βGAO unit cell has 10 atoms that generate 30 normal modes of vibration, 3 acoustic and 27 optical[7]. In this work we will be concerned with the effects of these phonons on conductivity. Acoustic phonons scatter electrons elastically, or nearly so, and can affect μ in degenerate semiconductors at low temperatures[14]. However, they will have negligible effect on electron phase and thus will not influence $\Delta\sigma$. Optical phonons, on the other hand, lead to inelastic scattering and will have a strong effect on $\Delta\sigma$[11–13]. They will also affect μ, but only at higher temperatures because temperature-independent ionized-impurity scattering, an elastic process, is much stronger than phonon scattering at low temperatures in highly-doped materials.

The random positions of the Si ions lead to a disorder that can result in a partial localization of the phonon and electron structures, known sometimes as "weak localization"[11,12]. Indeed, this disorder is the origin of the $\Delta\sigma$ measured here. To first order, it is customary to express the altered phonon spectrum as a somewhat localized superposition of the normal modes[12]. In the spirit of that approximation, our approach here will be to find an *effective* value of T_{po} at each temperature, i.e., $T_{po}(T)$, that can correctly describe optical-phonon scattering in three independent experiments: $\Delta\sigma$ vs T, $\Delta\sigma$ vs B, and μ_H vs T.

Transport in both bulk and thin-film βGAO has been studied by several groups in the recent past[8,10,16,17]. Ma *et al.*[16] demonstrated the critical mobility-limiting role of polar-optical phonons by analyzing μ vs T at $n \sim 10^{17}$ cm^{-3}, and also μ vs n at $n \sim 10^{16}$–10^{19} cm^{-3} and at T ~ 77 K and 300 K. Among other things, they found that an effective value of $kT_{po} \approx 44$ meV (511 K) gave a reasonable fit to a compilation (literature) of μ vs n data at 300 K. Also, in bulk, nondegenerate βGAO, Oishi *et al.* found that the high-temperature mobility is controlled by a single effective T_{po}, although its value was unspecified[17]. Finally, Ghosh and Singisetti carried out a rigorous calculation of μ vs T for an ordered, nondegenerate sample with $n \sim 10^{17}$ cm^{-3}, and theory agreed well with experiment[8]. They included the effects of all the individual optical phonons and found that phonons of different energies and polarizations affected the scattering in different ways at different temperatures. For example, an optical phonon of energy ≈ 21 meV ($T_{po} \approx 244$ K) dominated the mobility at 300 K[8]. At lower temperatures, other optical phonons became important and of course it was also necessary to add the scattering contributions of acoustic phonons and ionized impurities. In another theoretical work, Kang *et al.*[10] performed first-principles calculations on the electron and phonon structures and also calculated scattering rates and mobilities. In agreement with the conclusions of Ghosh and Singisetti[8], they showed that many phonons contribute to the scattering. Moreover, they pointed out the dominance of polar vs nonpolar optical scattering and showed that, contrary to other assertions, the mobility does not have a large anisotropy. In principal, detailed and rigorous calculations such as those described above could be carried out for all lightly-doped, ordered βGAO samples; however, the disorder arising from heavily-doped samples will modify the actual phonon spectrum and require a more complicated analysis[12].

We first consider the classical theory of μ vs T in degenerate semiconductors, standard in the literature[18] except for the treatment of optical-phonon scattering. (In the equations below, the effective mass m*, static dielectric constant ε_0, and high-frequency dielectric constant ε_1 were taken from ref.[7] and the acoustic deformation constant E_1 and longitudinal elastic constant c_l from ref.[16], noting that $c_l = \rho_{dens} s^2$, where ρ_{dens} is the mass density and s is the speed of sound. The only fitted parameter in our study is T_{po}.) For degenerate materials, the dominant scattering mechanisms are typically ionized impurities ("ii"), acoustic phonons ("ac"), and optical phonons ("po"). The existence of degeneracy greatly simplifies the calculations, because all scattering basically occurs at one energy, the Fermi energy, $E_F = (\hbar^2/2\,m^*)(3\pi^2 n)^{2/3}$, where ħ is the reduced Planck's constant. For degenerate electrons, Matthiessen's Rule[14,18] applies exactly:

$$\mu(n, N_D, N_A, T) = \left[\mu_{ii}(n, N_D, N_A)^{-1} + \mu_{ac}(n, T)^{-1} + \mu_{po}(n, T)^{-1}\right]^{-1} \quad (1)$$

We will assume that the dominant donor has charge Z_D, and the acceptor, Z_A; then $n = Z_D N_D - Z_A N_A$[18]. In our case, the dominant donor is the dopant Si_{Ga}, with $Z_D = 1$. The form of Eq. 1 assumes that a relaxation time τ can

be defined for each scattering mechanism, i.e., $\mu = e\tau/m^*$. This criterion holds for elastic scattering (ii and ac) but not necessarily for inelastic scattering (po), discussed further below. From the degenerate Brooks-Herring ionized-impurity scattering theory[14], μ_{ii} can be written

$$\mu_{ii}(n) = \frac{24\pi^3\varepsilon_0{}^2\hbar^3}{e^3(m^*)^2}\frac{1}{\ln(1+y(n)) - \frac{y(n)}{1+y(n)}}\frac{n}{Z^2N_{ii}} \tag{2}$$

where $Z^2N_{ii} \equiv N_{ii,eff} = Z_D{}^2N_D + Z_A{}^2N_A$, where $N_{ii,eff}$ is the *effective* concentration of ionized impurities[18]. [Note that $N_{ii,eff}$ is the only fitted parameter in Eq. 2, and from it we can calculate N_D and N_A: $N_D = (N_{ii,eff} + nZ_A)/(1 + Z_A)$ and $N_A = (N_{ii,eff} - n)/ Z_A (1 + Z_A)$.] In Eq. 2, y(n) can be written[14]

$$y(n) = \frac{3^{1/3}4\pi^{8/3}\varepsilon_0\hbar^2n^{1/3}}{e^2m^*} \tag{3}$$

The other two scattering terms in Eq. 1 are:

$$\mu_{ac}(n, T) = \frac{\pi\hbar^4c_l}{2^{1/2}(m^*)^{5/2}E_1{}^2ekT}E_f(n)^{-1/2} = \frac{\pi^{1/3}\hbar^3c_l}{3^{1/3}m^{*2}E_1{}^2ekTn^{1/3}} \tag{4}$$

$$\mu_{po}(T) = \frac{4\pi\varepsilon_0(3/\pi)^{1/3}\hbar^3n^{1/3}T\sinh^2\left(\frac{T_{po}}{2T}\right)}{ekT_{po}{}^2(m^*)^2(\varepsilon_0/\varepsilon_1 - 1)} \tag{5}$$

Equation 4 is well-known[18], but Eq. 5 is not in the literature, to our knowledge. To derive Eq. 5, we begin with Eq. 17 in the theoretical paper[19] of Howarth and Sondheimer (HS). These authors use a variational theory to show that even for polar optical phonon scattering a relaxation time $\tau(E)$ can be defined as long as $T > T_{po}$. This is an important result, but HS-Eq. 17 can be made more useful by including the concept of an effective charge, introduced earlier for materials that have partially-ionic/partially-covalent bonds[20,21]. We make use of the Callen effective charge $e_c{}^2$[20], which can be written as $e_c{}^2 = (kT_{po}/\hbar)^2(\varepsilon_0/\varepsilon_1 - 1)M_ra^3$, where M_r is the reduced ion mass and a^3 is the volume of the unit cell. (It turns out that both M_r and a^3 cancel out in the final equation.) Besides substituting $e_c{}^2$ for e^2 we multiply HS-Eq. 17 by $4\pi\varepsilon_0$ for conversion to MKS units.

For degenerate electrons, in which case scattering occurs only at the Fermi energy, Eq. 5 gives $\tau \propto n^{1/3}$, a relationship also noted in earlier work[22]. For lower temperatures, i.e., $T < T_{po}$, Eq. 5 must be corrected according to a table provided by HS[19]. For our calculated values of T_{po}/T, shown below to range from about 5–10, the corrections are less than about 20%. Therefore, we will assume the approximate validity of Eq. 5 in order to maintain simplicity and convenience. This assumption is partially justified by the fact that Eqns. 2–5 fit the experimental mobility data quite well, as shown in Fig. 2.

We next consider the quantum-based magnetoconductivity, $\Delta\sigma(B,T)$. Conductivity in disordered materials is affected by the wave nature of the electrons as they diffuse and scatter from point to point. This process is perhaps best understood in terms of Feynman's approach to quantum mechanics, the path integral method. An electron diffusing from point A to point B may have many potential paths, all of which must be included in a sum of amplitudes. Even if coherence is maintained, the phases in general will not add constructively because the travel distances will vary. However, there are some paths, those containing loops, for which a portion of the travel can generate constructive interference. That is, one path can have the electron traversing in one direction around the loop, and a second path, in the other direction. Since exactly the same travel distance will occur for each, they will interfere constructively and thus be more probable than a similar path without a loop. Therefore, paths with loops are favored, and they will generate a certain amount of "backscattering" of the electron, which will reduce conductance. (This effect is not large; for our sample $\Delta\sigma/\sigma \approx 0.004$ at T = 9 K and B = 10 kG.) All of the discussion so far assumes that coherence is maintained during the loop travel, which is true if all of the scattering is elastic. However, as temperature is increased, inelastic scattering from the optical phonons will begin to affect the electron energy and randomize its phase. Also, the presence of a magnetic field will affect phase. Both of these effects are quantified in the 3D perturbation theory of Kawabata[13]:

$$\Delta\sigma(B, T) = \frac{e^2}{2\pi^2\hbar l(B)}\sum_{N=0}^{\infty}2[(N+1+\delta(B,T))^{1/2} - (N+\delta(B,T))^{1/2}] - \frac{1}{\left(N+\frac{1}{2}+\delta(B,T)\right)^{1/2}} \tag{6}$$

where $e^2/2\pi^2\hbar = 1.23 \times 10^{-5}$ S, is the so-called unit of quantum conductance. Also, $l(B) = (\hbar/eB)^{1/2}$ and

$$\delta(B, T) = \frac{l^2(B)}{4\tau_{po}(T)D(T)} = \frac{3e}{4\hbar(3\pi^2n)^{2/3}\mu_{po}(T)\mu(T)B} \tag{7}$$

where τ_{po} is the inelastic-scattering relaxation time and D(T) is the diffusion coefficient. We have modified Eq. 7 by setting $\tau_{po} = m^*\mu_{po}/e$ and $D = v_F{}^2\tau/3 = \hbar^2(3\pi^2n)^{2/3}\mu/3em^*$, where μ_{po} is given by Eq. 5 and n and μ are measured quantities. A remarkable consequence of Eq. 6 occurs in the limit of low T (which gives high μ_{po}) and large B which renders $\delta \ll 1$ and

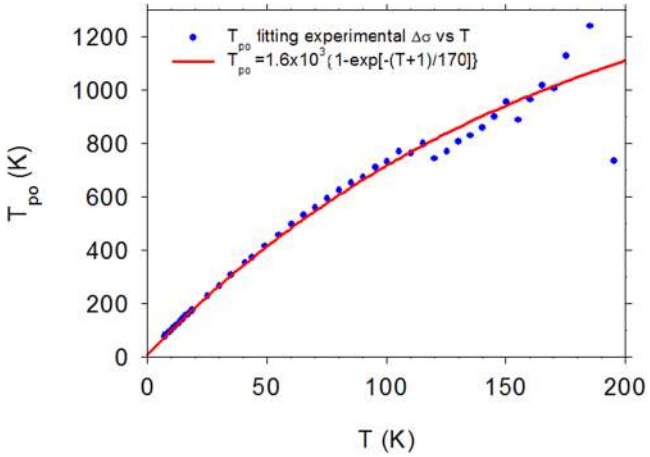

Figure 4. Experimental points: the required value of T_{po} to fit $\Delta\sigma$ vs T, B = 10 kG, at *each* temperature T, for βGAO. Solid line: a fit of T_{po} vs T, giving $T_{po}(T) = 1.6 \times 10^3\{1 - \exp[-(T + 1)/170]\}$ K.

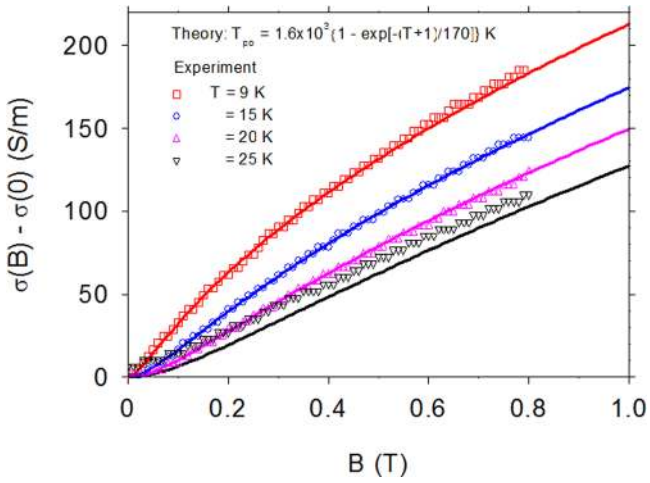

Figure 5. Experimental points: magnetoconductivty $\Delta\sigma = \sigma(B) - \sigma(0)$ at temperatures T = 9, 15, 20, and 25 K. Solid lines: theoretical fits with $T_{po}(T) = 1.6 \times 10^3\{1 - \exp[-(T + 1)/170]\}$ K.

$$\Delta\sigma(B,\ T) = \frac{0.605e^2}{2\pi^2\hbar l(B)} = \frac{0.605e^{5/2}}{2\pi^2\hbar^{3/2}}B^{1/2} = 290.8B^{1/2}S/m \tag{8}$$

This result is independent of temperature or any material parameter!

Equation 6 is applied to experimental results for βGAO in Fig. 3, which displays $\Delta\sigma$ vs T at B = 10 kG. It is instructive to compare the same function in thin-film, degenerate ScN. Note that ScN has only two atoms per unit cell and thus only one optical branch, which can be represented by a single value of T_{po}. As seen in Fig. 3, the value $T_{po} = 550$ K fits the ScN data very well. (A more detailed study of magnetoconductance in ScN will be presented elsewhere.) However, a single T_{po} is not sufficient for βGAO, and indeed, we find the required T_{po}, at a given T, by solving Eq. 6 as a transcendental equation with T_{po} as the unknown. The resulting points T_{po} vs T are plotted in Fig. 4, and they can be reasonably well fitted by the relatively simple function $T_{po}(T) = 1.6 \times 10^3\{1 - \exp[-(T + 1)/170]\}$ K, shown as a solid line. The validity of this equation can then be further tested via an independent experiment, $\Delta\sigma(B, T) = \sigma(B, T) - \sigma(0,T)$ vs B, B = 0–8 kG, T = 9, 15, 20, and 25 K. (For this particular experiment, 8 kG was the maximum field that could be used.) As seen in Fig. 5, the fit is excellent for T = 9, 15, and 20 K, and acceptable for T = 25 K, where the signal is rapidly decreasing due to inelastic scattering.

The final test of $T_{po}(T)$ is its applicability in a third independent experiment, μ_H vs T, illustrated in Fig. 2. Here we apply Eqns 1–5, comparing three choices of T_{po} in Eq. 5: 1000 K, 1400 K, or our derived function $T_{po}(T)$. The first two values were chosen to bracket the potential fits attained with T_{po} = constant; however, neither is satisfactory, nor is any other constant value. On the other hand, the function $T_{po}(T)$ works very well. We are now left with only one unknown in Eqns 1–5, $N_{ii,eff}$, which turns out to be 5.97×10^{20} cm^{-3} from the solid-line fit shown in Fig. 2. We know that the dominant donor concentration $N_D = [Si_{Ga}]$, and we can speculate that the dominant acceptor is the Ga vacancy, V_{Ga}[23,24]. The latter, if isolated, would have a charge $Z_A = 3$, but if complexed with Si, Z_A could be 2, or even 1. As shown earlier, we can then calculate N_D and N_A from $N_{ii,eff}$. Under the

assumptions, $Z_D = 1$ and $Z_A = 1$, 2, or 3, the results are: $N_D = 3.57$, 2.77, or $2.37 \times 10^{20}\,cm^{-3}$; and $N_A = 2.40$, 0.80, or $0.40 \times 10^{20}\,cm^{-3}$, respectively. To decide among these three possibilities it would be helpful to determine [Si] from another source, such as secondary ion mass spectroscopy, and $[V_{Ga}]$ from positron annihilation or electron paramagnetic resonance.

In summary, we have used the quantum-based magnetoconductivity $\Delta\sigma$ vs T to develop a function $T_{po}(T)$ that quantitatively explains not only $\Delta\sigma$ vs T but also $\Delta\sigma$ vs B and μ_H vs T in degenerate βGa_2O_3. We also showed that the behavior of σ, $\Delta\sigma$, and μ_H in βGa_2O_3 is much different than that in ScN, a simpler system for which a *constant* T_{po} well explains both $\Delta\sigma$ vs T and μ_H vs T. The methodology used to develop the function $T_{po}(T)$ is directly applicable to other complex semiconductors.

References

1. Higashiwaki, M. & Jessen, G. H. Guest Editorial: The dawn of gallium oxide microelectronics. *Appl. Phys. Lett.* **112**, 060401 (2018).
2. Baldini, M., Galazka, Z. & Wagner, G. Recent progress in the growth of β-Ga_2O_3 for power electronics applications. *Mater. Sci. in Semiconductor Processing* **78**, 132–146 (2018).
3. Green, A. *et al.* 3.8-MV/cm breakdown strength of MOVPE-grown Sn-doped β-Ga_2O_3 MOSFETs. *IEEE Electron Device Letters* **37**, 902–905 (2016).
4. Leedy, K. D. *et al.* Highly conductive homoepitaxial Si-doped Ga_2O_3 films on (010) β-Ga_2O_3 by pulsed laser deposition. *Appl. Phys. Lett.* **111**, 012103 (2017).
5. Xia, Z. *et al.* Delta Doped β-Ga_2O_3 Field Effect Transistors With Regrown Ohmic Contacts. *IEEE Electron Device Letters* **39**, 568–571 (2018).
6. Rode, D. L. Low-field Electron Transport. *Semiconductors and Semimetals* **10**, 1–89, (cf. Table on p. 84.) (1975).
7. Schubert, M. *et al.* Anisotropy, phonon modes, and free charge carrier parameters in monoclinic β-gallium oxide single crystals. *Phys. Rev. B* **93**, 125209 (2016).
8. Ghosh, K. & Singisetti, U. *Ab initio* calculation of electron-phonon coupling in monoclinic β-Ga_2O_3 crystal. *Appl. Phys. Lett.* **109**, 072102 (2016).
9. Sturm, C., Schmidt-Grund, R., Zviagin, V. & Grundmann, M. Temperature dependence of the dielectric tensor of monoclinic Ga_2O_3 single crystals in the spectral range 1.0−8.5 eV. *Appl. Phys. Lett.* **111**, 082102 (2017).
10. Kang, Y., Krishnaswamy, Y. K., Peelaers, H. & Van de Walle, C. G. Fundamental limits on the electron mobility of β-Ga_2O_3. *J. Phys. Condens. Matter* **29**, 234001 (2017).
11. Lee, P. A. & Ramakrishnan, T. V. Disordered electronic systems. *Rev. Modern Phys.* **57**, 287–337 (1985).
12. Dugdale, J. S. *The Electrical Properties of Disordered Metals* (Cambridge University Press, Cambridge, 2005).
13. Kawabata, A. Theory of Negative Magnetoresistance in Three-Dimensional Systems. *Solid State Commun.* **34**, 431–432 (1980).
14. Look, D. C. Electrical Characterization of GaAs Materials and Devices (Wiley, New York, 1989).
15. Look, D. C., Wang, B. & Leedy, K. D. Model-free determination of optical constants: application to undoped and Ga-doped ZnO. *Opt. Eng.* **56**, 034112 (2017).
16. Ma, N. *et al.* Intrinsic electron mobility limits in β-Ga_2O_3. *Appl. Phys. Lett.* **109**, 212101 (2016).
17. Oishi, T., Koga, Y., Harada, K. & Kasu, M. High-mobility β-Ga_2O_3(-201) single crystals grown by edge-defined film-fed growth method and their Schottky barrier diodes with Ni contact. *Appl. Phys. Express* **8**, 031101 (2015).
18. Look, D. C. *et al.* Self-compensation in semiconductors: The Zn vacancy in Ga-doped ZnO. *Phys. Rev. B* **84**, 115202 (2011).
19. Howarth, D. J. & Sondheimer, E. H. The theory of electronic conduction in polar semiconductors. *Proc. Roy. Soc. A* **219**, 53–74 (1953).
20. Callen, H. B. Electric Breakdown in IonicCrystals. *Phys. Rev.* **76**, 1394–1402 (1949).
21. Böer, K.W. *Survey of Semiconductor Physics* (Van Nostrand Reinhold, New York, 1990).
22. Zawadzki, W. & Szymanska, W. Phys. Stat. *Solidi B* **45**, 415 (1971).
23. Korhonen, E. *et al.* Electrical compensation by Ga vacancies in Ga_2O_3 thin films. *Appl. Phys. Lett.* **106**, 242103 (2015).
24. Kananen, B. E., Halliburton, L. E., Stevens, K. T., Foundos, G. K. & Giles, N. C. Gallium vacancies in β-Ga_2O_3 crystals. *Appl. Phys. Lett.* **110**, 202104 (2017).

Acknowledgements

This material is based upon work supported in part by the Air Force Office of Scientific Research under award number FA9550- RY18COR098. Further financial support was provided by the Air Force Research Laboratory under Contract FA8075-14-D-0025 and the National Science Foundation under grant DMR-1800139 (T. Paskova). We wish to thank T.A. Cooper, W. Rice, and D. McFarland, for critical technical support in these experiments. We also are grateful to Dr. A.N. Reed for permission to use the ScN data of Fig. 3.

Author Contributions

D.C.L. and K.D.L. designed and directed this study. D.C.L. carried out the electrical, optical, and theoretical analysis. K.D.L. developed the degenerate, homoepitaxial layer growth. Both authors contributed to writing the manuscript.

Additional Information

Competing Interests: The authors declare no competing interests.

Publisher's note: Springer Nature remains neutral with regard to jurisdictional claims in published maps and institutional affiliations.